Article ID: 1006-8775(2011) 02-0156-10

CHARACTERISTICS OF INTENSITY CHANGE IN TROPICAL CYCLONES AFFECTING THE SOUTH CHINA SEA FROM 1977 TO 2007

LI Xun (李 勋)[1], ZHAO Sheng-rong (赵声蓉)[2], LI Ze-chun (李泽椿)[2], LI Ying (李 英)[3], WANG Yong (王勇)[4]

(1. Hainan Province Meteorological Observation, Haikou 570203 China; 2. National Meteorological Center, China Meteorological Administration, Beijing 100081 China; 3. Chinese Academy of Meteorological Sciences, Beijing 100081 China; 4. Nanjing University of Information Science & Technology, Nanjing 210044 China)

Abstract: The best track data of tropical cyclones (TCs) provided by Regional Specialized Meteorological Center (RSMC) Tokyo for the South China Sea (SCS) from 1977 to 2007 are employed to study the spatiotemporal variations (for a period of 12 hours) and the rapid (slow) intensification (RI/SI) of TCs with different intensity. The main results are as follows. (1) Over this period, the tropical storms (TSs) and severe tropical storms (STSs) mostly intensify or are steady while the typhoons (TYs) mostly weaken. The stronger a TC is initially, the more observation of its intensification and the less its variability will be; the more observation of its weakening is, the larger its variability will be. (2) The TC intensifies the fastest at 0000 UTC while weakening the fastest at 1200 UTC. (3) In the intensifying state, TSs, STSs, and TYs are mainly active in the northeastern, central-eastern, and central SCS respectively. The weakening cases mainly distribute over waters east off Hainan Island and Vietnam and west off the Philippines. Some cases of TSs and STSs weaken over the central SCS. (4) The RI cases form farther south in contrast to the SI cases. The RI cases are observed in regions where there are weaker vertical shear and easterly components at 200 hPa. The RI cases also have stronger mid-and lower-level warm-core structure and smaller radii of 15.4 m/s winds. The SI cases have slightly higher SST.

Key words: tropical cyclones; statistics; intensity; South China Sea

CLC number: P444 **Document code:** A **doi:** 10.3969/j.issn.1006-8775.2011.02.008

1 INTRODUCTION

As China is one of the countries in the world that is subject to most severe impacts of tropical cyclones (TCs)[1], accurate TC intensity forecasts are indispensable for people to take precautions to mitigate the loss inflicted by TCs[2]. Understanding of the statistics of intensity change in TCs is the basis of improving the capabilities of forecasting the TC intensity[3]. Based on datasets of 35 years and 55 years respectively, Yu et al.[3] and Yu et al.[4] defined changes in center pressure in subsequent 6 hours at every measurement time as the changes in TC intensity and studied the statistics of TC intensity change in the northwestern Pacific. Li et al.[5] summarized a number of characteristics of the TCs making landfall in China. Yuan et al.[6] made an intensive study on the spatial and temporal distribution of northwestern Pacific TCs with different intensity over a period of 60 years. According to Chen et al.[1], TC intensity changes can be divided into two types, one being slow changes, as found in most cases and the other being rapid changes, as found in some cases. Failure in forecast is mainly due to rapid intensification (RI) of the TC[7]. The eyes of the TCs experiencing RI are usually small, as indicated in some studies on the statistics of the northwestern Pacific TCs with RI in offshore waters of China and associated large-scale circulation[8, 9]; they are mainly affected by low-latitude circulation and synoptic systems[10] and usually occur at 15–20° N and coastal areas of Zhejiang, Fujian, Guangdong and Guangxi and the Philippines Sea to the east of the Bashi Channel[11]. Factors like warm sea surface temperature (SST)[8, 12-14], increased kinetic energy from low-level rotational wind[15], developed cumulus convection[16], and Tropical Upper Tropospheric Trough (TUTT)[12,

Received 2010-06-25; **Revised** 2011-03-03; **Accepted** 2011-04-15
Foundation item: Specialized Project for Forecasters, China Meteorological Administration 2011 (CMAYBY2011-041)
Biography: LI Xun, Ph. D., primarily undertaking research on tropical cyclones.
Corresponding author: LI Xun, e-mail: cyrilpat@sina.com

17] may contribute to the appearance of RI. For causes other than those presented above, mild cold air from the north streaming southward into the TC prior to landfall can affect its thermodynamic structure so that geopotential instability is strengthened, as shown in a diagnostic study of TC Vongfong that intensified offshore[18]. TCs that abruptly intensify have the potential of primary development, as indicated in a study on the large-scale characteristics of TCs that abruptly change intensity prior to landfall in the south of China (Hu et al.[19]). An intensifying TC has the smallest average radius of wind, a conclusion made in a study of the TC scale statistics in the northwestern Pacific using the radii of 15.4 m/s and 25.7 m/s winds, respectively.

On average, mean intensity of TCs in central SCS does not vary much[3], with most of the TCs evolving slowly and a few of them developing rapidly. Research is not common on contrastive comparison between the RI and SI cases in the SCS, though attempts by Yuan et al.[6] are useful in investigating into the characteristics of intensity change in TCs of different intensity over the northwestern Pacific. Using the data of TCs for 1977–2007 (a total of 31 years), this work measures the intensity change based on 12-h changes in the maximum wind speed near the eye, studies how TCs of varying intensity in the SCS change in intensity over a certain period of time (12 h) and the large-scale statistics of RI and SI cases, so as to increase the understanding of the variation of intensity in TCs that affect the SCS.

2 DATA AND METHODS

TC intensity is usually depicted in terms of minimum sea level pressure or maximum wind speed near the eye (referred to as the "maximum wind speed" hereafter)[3]. At present, the maximum wind speed is used to categorize the intensity of TCs into tropical depressions, tropical storms, severe tropical storms, typhoons, and severe typhoons[21]. In their work on studying and comparing the datasets of three major forecasting centers in Northwest Pacific, the China Meteorological Administration (CMA), Regional Specialized Meteorological Center (RSMC) Tokyo, and Joint Typhoon Warning Center (JTWC), Yu et al.[22] concluded, following the method of climatological persistence, that RSMC has the least root mean square errors. Yuan et al.[20] also argued that the data offered by RSMC have the best reliability for it is part of an observational program of the World Meteorological Organization. That is why all of the radii of 15.4 m/s winds in this work are from the RSMC.

RSMC offers data four times a day at 0000 UTC, 0600 UTC, 1200 UTC, and 1800 UTC. The maximum wind speed began to be measured from 1977. To study the variation tendency or variability of the TC intensity, the variation of the maximum wind speed from the initial time (t = 0 h) to the point 12 hours afterwards is expressed as ΔV_{12}. When $\Delta V_{12}>0$ m/s, the TC is strengthened; when $\Delta V_{12}<0$ m/s, the TC is weakened; when $\Delta V_{12}=0$, the TC is stable in intensity. As the dataset does not include the wind speed of TD and the sample is relatively small for STY in the SCS[6], our work includes the TS, STS, and TY in studying the tendency of TC intensity change. According to the specifications for categorizing TC intensity that were first applied in June 2006 in China[6], this work classifies the TC into three groups based on the value of maximum wind speed (Table 1). With land cases removed, the total sample comprises 1703 TCs. The NCEP/NCAR reanalysis (2.5° ×2.5°)[23], available four times daily, and weekly mean SST reanalysis[24], provided by U.S. NOAA, make up the rest of the data studied. The t-test method is used to see if significant differences exist between the RI and SI cases in the large-scale statistical characteristics at the initial time (t = 0 h).

Table 1. Categorization of TC intensity and size of samples

Initial intensity	Wind speed /(m/s)	Sample size
All TCs	≥17.2	1703
TS	17.2～24.4	705
STS	24.5～32.6	559
TY	≥32.7	439

3 STATISTICS OF INTENSITY CHANGE IN TCS

3.1 *A number of statistic quantities*

Table 2 presents the number of observation and statistics of TCs with different intensity in the strengthening, weakening and stable states in 1977–2007. The TS has the most number of observation and an average intensification rate of 4.12 (m/s)/12 h; the TY has the most number of observation and an average weakening rate of -4.64 (m/s)/ 12 h. Under stable condition, the higher the number of TS observation, the smaller the number of STS. In a word, the less the number of observation of strong initial intensity, the larger the number of observation of TC weakening and the larger the variability.

Besides, the maximum of ΔV_{12} increase occurred at 0000 UTC (Coordinated Universal Time, same below) on 29 September 1983 with Georgia, a TS (also known as 8311 in the international code, same below) that was located at 19.3° N, 114.9° E with a ΔV_{12} increase of 17.99 m/s. The minimum of ΔV_{12} decrease happened at 0600 UTC on 11 November 2001 with Lingling (0123), a TY that was located at 13.5° N, 111.7° E with a ΔV_{12} decrease of 17.99 m/s.

Table 2. Statistics of intensity change in TCs with different intensity

	TC	TS	STS	TY
Samples of intensification	678（39.8%）	334（47.4%）	228（40.8%）	116（26.4%）
Samples of weakening	402（23.6%）	79（11.2%）	152（27.2%）	171（39%）
Samples of stabilization	623（36.6%）	292（41.4%）	179（32.0%）	152（34.6%）
Mean intensification rate/(m·s^{-1}/12 h)	3.95	4.12	3.88	3.61
Standard deviation of intensification rate/(m·s^{-1}/12 h)	2.11	2.32	1.98	1.62
Mean weakening rate/(m·s^{-1}/12 h)	−4.17	−3.22	−4.14	−4.64
Standard deviation of weakening rate/(m·s^{-1}/12 h)	2.31	1.12	2.11	2.72

Figure 1 shows the frequency of ΔV_{12} for TCs of different intensity. ΔV_{12} varies between -2.57 m/s and 2.57 m/s, suggesting a mild intensity variability over most of the life cycle of TCs[3]. Under the strengthening state, the sample with the initial intensity of TS is the largest, followed by STS, which is consistent with the results of Table 2. It may be attributable to the fact that relatively weak TCs are more likely to strengthen for they are well below the maximum possible intensity (MPI)[14]. In the weakening state, the sample with the initial intensity of TY is the largest, followed by STS, possibly because intense TCs tend to weaken due to the collapse of the eyewall[14].

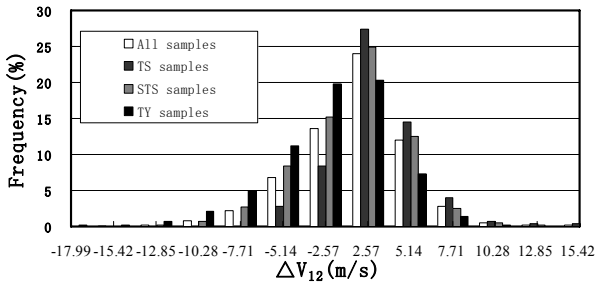

Fig. 1. Distribution of frequency (%) of intensity change in TCs with different initial intensity

3.2 *Monthly distribution*

Figure 2 presents the monthly number and total number of TC cases with different initial intensity corresponding to the strengthening and weakening state, respectively. It is shown that June to November is the most active TC season in the year (Fig. 2a). All types of strengthening cases are increasing consistently from January to September, with the number of TS being the most and that of TY the least. The peaks of TS and STS appear in September. Except for TY, all other strengthening cases are gradually decreasing after September. The number of strengthening TY cases increases significantly in August–October, with the peak in October and an average of 39 cases; the number begins to decline after October.

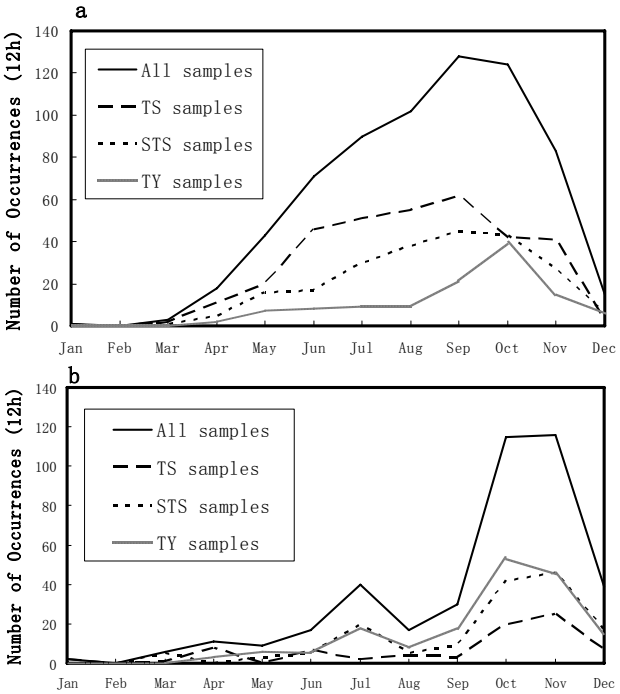

Fig. 2. Monthly mean number of cases of TCs in terms of intensity change for different initial intensity corresponding to the strengthening (a) and weakening (b) states

Due to relatively small size of cases for January to March (Fig. 2), the percentages of the observation of TCs for different initial intensity are presented in Fig. 3 that correspond to the strengthening cases (a) and weakening cases (b) in April to December (Fig. 3a). It is shown that the TS in April to September and November take up the most percentage (more than 46%) and the TY the least (generally lower than 20%). The case of December is just the opposite, with the TY having the highest portion (40%) and the TS the lowest portion (20%). For October, the percentage of STS is the highest (34.7%), a little higher than that of TS (33.9%). In the weakening state (Fig. 3b), the TY has the highest percentage (more than 40%), followed by STS, while the TS in April and June have higher percentages, being 72.7% and 41.8%, respectively.

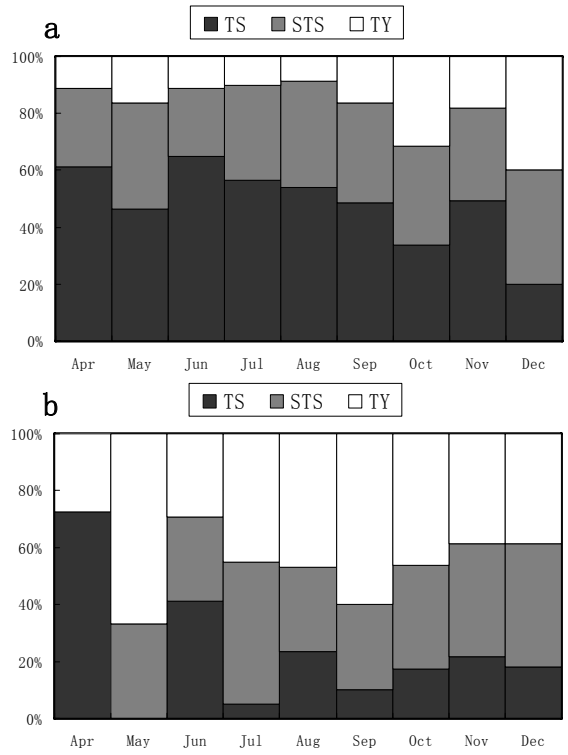

Fig. 3. Monthly percentages of intensity change (within 12 hours) of TCs with different initial intensity in the strengthening (a) and weakening (b) states

3.3 *Diurnal variation*

Examining the average number and strengthening rate of the TCs in the strengthening cases (Table 3) and weakening cases (Table 4) for four times of daily measurement, this paper discovered that the sample for all TCs has the highest rate of intensification, 4.17 (m/s)/12 h, at 0000 UTC and is the largest in size, 180 in all, followed by 1800 UTC with 1.17 (m/s)/12 h and a size of 179, and further by 1200 UTC with 3.71 (m/s)/12 h. Differences exist in the diurnal variation of TCs with different initial intensity; 0000 UTC marks the time with the largest rate of strengthening (4.43 (m/s)/12 h)) and 1800 UTC sees the largest rate of strengthening (4.08 (m/s)/12 h). In contrast, the TY has the highest rate of strengthening at 1200 UTC (3.70 (m/s)/12 h) and a slightly smaller size of 25 while having the most number at 0000 UTC and a strengthening rate of 3.69 (m/s)/12 h, which is very close to that of 1200 UTC. The highest rate of weakening happens at 0600 UTC with the TY (-4.76 (m/s)/12 h) and the lowest at 0000 UTC with the TS (-2.87 (m/s)/12 h), which is actually its initial intensity. In summary, the greater the initial intensity, the larger the rate of weakening; the weakening rate of the TY is larger than that of either the TS or the STS.

Table 3. Numbers and strengthening rates of TCs averaged over all time of measurement under different initial intensity (Unit inside the parenthesis: m s^{-1}/12 h)

Time of measurement/h	TC number (strengthening rate)	TS number (strengthening rate)	STS number (strengthening rate)	TY number (strengthening rate)
00	180(4.17)	83(4.43)	65(4.07)	32(3.69)
06	158(3.74)	70(4.00)	57(3.56)	31(3.48)
12	160(3.71)	85(3.69)	50(3.75)	25(3.70)
18	179(4.13)	81(3.87)	56(4.08)	28(3.58)

Table 4. Same as Table 3 but for the numbers and weakening rates

Time of measurement/h	TC number (weakening rate)	TS number (weakening rate)	STS number (weakening rate)	TY number (weakening rate)
00	88(−3.94)	17(−2.87)	33(−3.58)	38(−4.73)
06	103(−4.14)	20(−3.08)	42(−4.04)	41(−4.76)
12	111(−4.45)	21(−3.55)	41(−4.64)	49(−4.67)
18	100(−4.11)	16(−4.66)	36(−4.21)	43(−4.42)

Units inside the parenthesis: m s^{-1}/12 h

3.4 *Regional distribution*

In determining the regional distribution of the cases, this paper gives the number of TC observation within each of the 1° ×1° longitude/latitude meshes for both the strengthening (Fig. 4) and weakening (Fig. 5) states in the TCs with varying intensity. It is seen that the sample is the largest with the TCs strengthening in northeast SCS (Fig. 4a), a result consistent with that of Yu and Yao[4] According to the observation by Yuan et al.[6], there are relatively a large number of TS and STS that form locally in the SCS or come from the northwest Pacific. In this study, the sample of strengthening TS in the SCS is the largest in size (Fig. 4c) while that of strengthening STS in the central and eastern SCS is the largest in size (Fig. 4d), indicating full development of the TCs in the SCS as they are far from land surface, like the islands of the Philippines. For the weakening case (Fig. 5a), it is mainly distributed over the ocean east of Hainan Island and Vietnam and the waters just west off the Philippines, reflecting the weakening role played by the land in reducing the TC intensity[3]. The weakening cases of the TS (Fig. 5b) and STS (Fig. 5c) have similar distribution; they are also present in central SCS in addition to the effect of land described above, which is similar to the results in Yu and Duan[3]. In

this study, however, it is the cases of the TS and STS that show the main reduction. In general, cases that weaken over the ocean surface mainly occur west of the high-value areas of strengthening cases while the weakening of the TY is mainly due to the land effect (Fig. 5d).

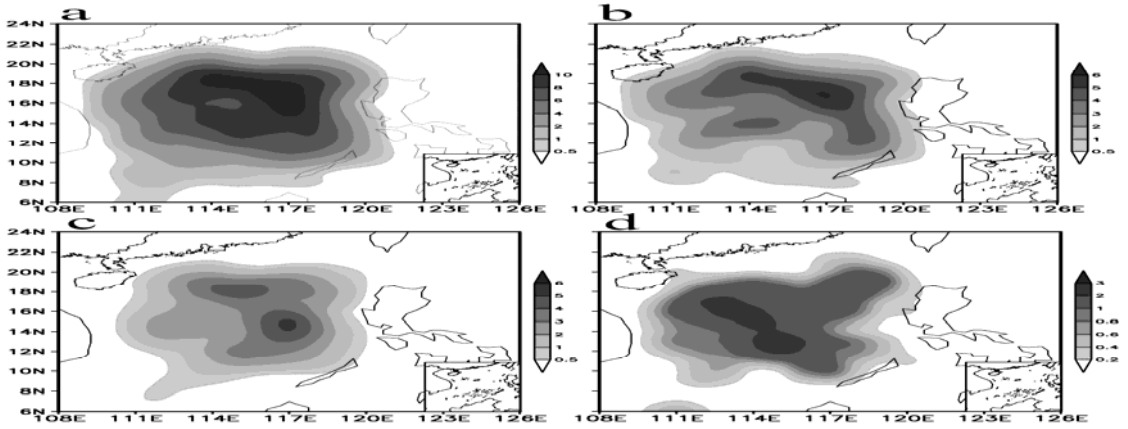

Fig. 4. Numbers of observation of all cases (a), TS (b), STS (c), and TY (d) for the strengthening TCs with different initial intensity

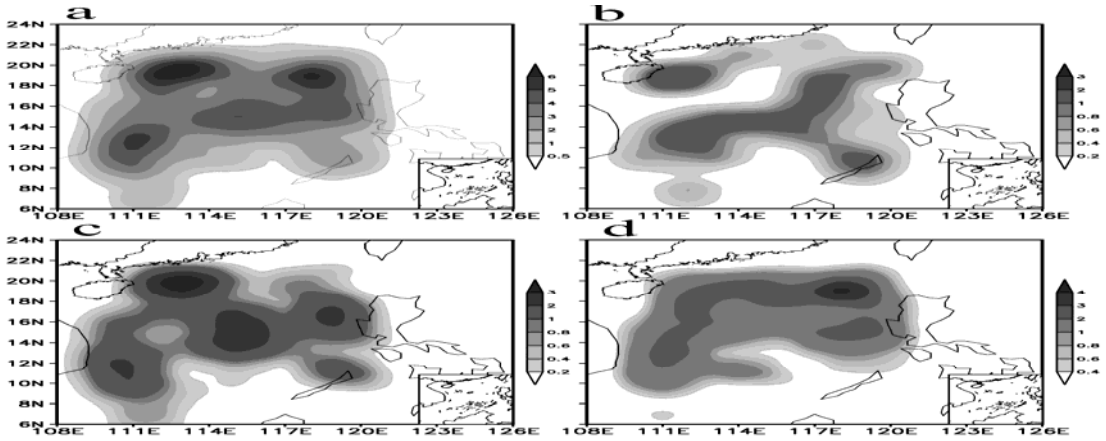

Fig. 5. Same as Fig. 4 but for the weakening TCs

4 STATISTICAL CHARACTERISTICS OF TCS WITH RI AND SI AT INITIAL TIME

4.1 *Accepted definition of RI and SI*

As what Yan et al.[21] have already pointed out, the center speed of TCs can now be determined using satellite data with the same effect as with air pressure. It is suggested in their work that the maximum wind speed of the center (shortened as MW hereafter) be used to define RI and set the increment of MW ≥10 (m/s)/12 h as the RI standard for offshore waters of China, based on the mathematical meaning of mean value and standard deviation. It is also suggested that the RI standard be adjusted in accordance with different initial intensity. Ventham and Wang[17] argued that it is necessary to distinguish the initial intensity in defining the standard of RI. Based on an accumulative frequency of MW increments, they set 30 kn/24 h (1 kn=0.54 m/s) as the standard of RI and 10 kn/24 h as that of SI for northwestern Pacific TCs with an initial intensity of 35 kn.

To study the statistical characteristics of RI in the SCS, the RI standard needs to be designed and samples need to be taken. Fig. 6 gives the accumulative frequency of ΔV_{12} increments for the TCs with different initial intensity, which shows that the TS sample intensifies the most, followed first by the STS sample, though with a mild difference, and then by the TY sample. This is a phenomenon that differs from the result that the TY in northwestern Pacific has the fastest intensification[17], possibly due to the fact that the relatively small area of the SCS does not facilitate the full development of the TY. For the TS, STS, and TY, the accumulative frequency of $\triangle V_{12}$≥7.7 m/s is 96.7%, 97.8% and 99.2%, respectively, showing close tendency in the intensity change of TS and STS.

Generally, RI is defined to appear when $\triangle V_{12}$ is greater than the average and standard deviations of the strengthening rate[21]. Table 2 shows that the sums of mean strengthening rates of TS, STS, and TY and their standard deviations are 6.44, 5.86, and 5.23 m

s^{-1}/12 h, respectively, and the accuracy of wind speed estimates is 5 kn (or 2.57 m/s). Therefore, RI can all be defined as $\triangle V_{12} \geq 7.71$ m/s, regardless of the difference in initial intensity, taking up 11.68%, 8.33% and 6.1% of the strengthening cases respectively. It is lower than the former standard of RI in China (≥10 m/s)[21] but close to that specified in Yu et al.(≥7.91 m/s)[26].

Cases would be limited if TCs of just one single category of initial intensity are taken into account. Yan et al.[21] pointed out that RI cannot be used in analysis or forecasting unless it is broadly based. As the TS and STS are similar in the distribution of the frequency of intensity change (Fig. 6), the TS and STS are studied in this work. For $\triangle V_{12} \geq 7.71$ m/s, there are a total of 58 RI cases. Fig. 7 gives the monthly distribution of the RI cases. It shows that the samples are relatively large in July, September and October, relatively small in March, April and May, but absent in the remaining months. As the rate of intensity change varies in a small range during most of the TC's life cycle, the initial intensity of ΔV_{12} = 2.57 m/s is defined as the standard of SI for the TS and STS, taking up 57.8% and 60.1% of the strengthening cases, respectively, and composing 332 cases in all.

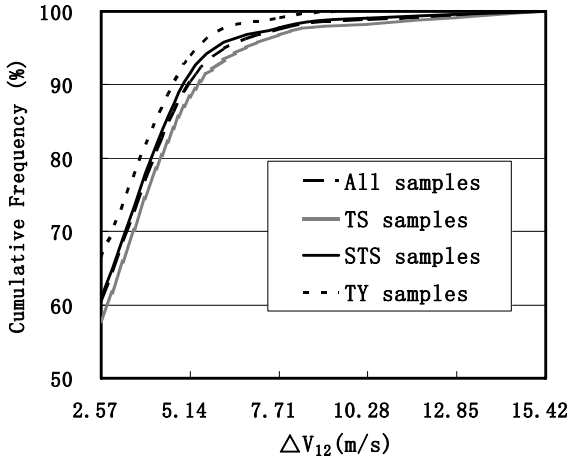

Fig. 6. Accumulative frequency of intensity change with different initial intensity (%)

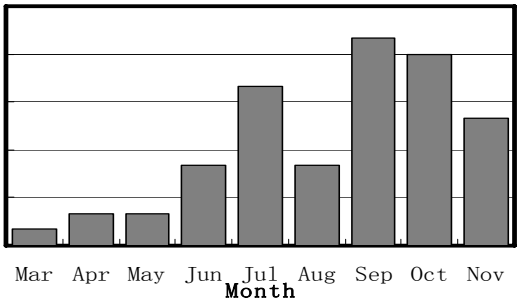

Fig. 7. Monthly distribution of the RI cases

4.2 *Statistical characteristics and frequency distribution of RI and SI for the initial time*

To compare the statistical characteristics of the RI and SI cases for the initial time (t = 0 h), the thermodynamic factors (i.e. SST, possible intensity and relative humidity near the low-level centre) and dynamic factors (i.e. 200-hPa zonal wind and wind vertical shear) as listed in Table 5 are selected, together with other factors like the latitude, longitude and the radius of the 15.4 m/s winds.

The weekly SST data from the National Oceanic and Atmospheric Administration (NOAA, USA) are linearly interpolated[27] and the spatial distribution of TC centers are treated with double linear interpolation. As the initial time of the SST data starts from October 29, 1981, the RI and SI cases of this factor drop accordingly at 53 and 285 respectively.

The maximum possible intensity (MPI) is computed in[14]

$$MPI = \min[X, 85] \tag{1}$$

where $X = A + B(\exp)[C(\mathrm{SST} - \mathrm{SST}_0)]$, A = 34.2 m/s, B = 55.8 m/s, C = 0.181 3/° C and SST_0 = 30° C

To show the potential capacity of TCs for development, the potential intensity, or POT[14], for the initial time of RI and SI (t = 0 h), is obtained by subtracting from MPI the maximum wind speed at t = 0 h ($V_{\max}$) so that

$$\mathrm{POT} = \mathrm{MPI} - V_{\max}(t = 0\,\mathrm{h}) \tag{2}$$

The domain for VWS (see Table 5 for the description of this and other abbreviations appearing in the current and subsequent paragraphs) computation varies from one study to another[27]. Averages of VWS for all gridpoints are taken within circles around the eye at a radius of 5° (lat./long.) in Zeng et al.[27] and Henley et al.[28], while averages of VWS are used for all gridpoints inside the circular ring formed between the radii of 200 km and 800 km from the eye (Kaplan and DeMaria)[14]. For the ease of comparison, this work follows the algorithm in Hanley et al.[28] to determine the VWS averages inside a 5° -radius circle around the eye, denoted VWS5, and the VWS averages inside a circular ring formed between a 2.5° -radius circle and a 7.5° -radius circle around the eye, denoted VWS7.

For the computation of 200-hPa zonal wind, the average is sought for the circular ring formed between a 2.5° -radius circle and a 7.5° -radius circle around the eye, denoted $U200$. For the relative humidity near the low-level eye, the average is obtained for the levels of 850 hPa to 700 hPa within the circular ring of the same radii near the eye, denoted RHLO. In the RSMC record of measurements, the 15.4 m/s wind radii, denoted $R15$, include the radii of both the long axis and short axis, and their average is taken in computation[20]. Table 6 presents the averages of individual factors (Table 5) and differences of the averages for the initial time of the

RI and SI cases. LAT, SST, *U*200 and VWS5 have passed the significance level of $\alpha=0.05$, VWS7 has passed that of $\alpha=0.01$, and *R*15 has passed that of $\alpha=0.001$, while LON, POT and RHLO all fail to pass the *t*-test at the $\alpha=0.05$ significance level.

Table 5. Factors used in statistic analysis of the RI and SI cases at the initial time ($t=0$ h)

Variables	Unit	Descriptions
LAT	° N	Latitude
LON	° E	Longitude
SST	° C	SST
POT	m/s	MPI minus maximum wind speed at initial time
*U*200	m/s	200-hPa zonal wind averaged over gridpoints inside circles at radii of 2.5° and 7.5° (lat./long.) from eye
VWS5	m/s	vertical shear averaged over gridpoints inside circles at radius of 5° from eye
VWS7	m/s	vertical shear averaged over gridpoints inside circles at radii of 2.5° and 7.5° from eye
RHLO	%	low-level (850–700 hPa) relative humidity near eye averaged over gridpoints inside circles at radii of 2.5° and 7.5° from eye
*R*15	Km	radius of 15.4 m/s wind circle

Table 6. Averages of individual factors and differences of the averages for the initial time of the RI and SI cases

Variables	Units	RI（$N=58$，$Ns=53$）	SI（$N=332$，$Ns=285$）	Diff. of averages（RI−SI）
LAT	° N	15.42	16.27	−0.85*
LON	° E	116.04	116.32	−0.28
SST	° C	28.30	28.57	−0.27*
POT	m/s	52.50	53.59	−1.09
*U*200	m/s	−4.67	−6.40	1.73**
VWS5	m/s	7.37	8.45	−1.08*
VWS7	m/s	6.95	8.60	−1.65**
RHLO	%	72.08	71.41	0.67
*R*15	Km	231.60	281.70	−50.1***

Note: *N* indicates the number of cases and *Ns* stands for the number of cases used for SST and POT analysis. The significance level of the *t*-test is $\alpha=0.05$*, $\alpha=0.01$**, and $\alpha=0.001$***, respectively.

Figure 8 gives the distribution of the frequency of averages of individual factors at the initial time of the RI and SI cases. It shows that the RI cases are located more southward in latitudes, with the difference of averages at -0.85° N (Table 6), and more westward in longitudes, than the SI cases (-0.28° E). It is clear from Fig. 8a that the RI cases located between 12° N and 14° N have the largest percentage (38%), followed by those between 18° N and 20° N (22%), suggesting the presence of considerable size of RI cases just offshore; the largest percentage of SI cases are found at 18–20° N, followed by those at 14–18° N. In a word, the RI mainly distributes at the low latitudes while the SI at the high latitudes.

According to the statistic results of Yuan et al.[20] on the climatology of SST in the northwest Pacific and SCS, the lower the latitude, the higher the SST. Compared to high latitudes, low latitudes are conducive to the development of RI, as pointed out by Kaplan and DeMaria[14]. It is, however, noteworthy that the average SST of RI and SI cases all surpass 28° C, though with the former being a little lower than the latter by a difference of -0.27° C in mean value; they have the highest frequency on the 28–29° C section of the SST (more than 50%, see Fig. 8c). As the SCS is a tropical sea, the SST differs only slightly; it is then a necessary rather than a decisive factor for RI in the SCS[8]. As there is no significant difference in the SST between the two kinds of cases, it is not hard to figure out why there is little difference in the calculated results of POT based on the SST.

As pointed out by Liang[29], the Intertropical Convective Zone (ITCZ) is an area where most heat and moisture are transported to serve as a source of energy of the tropics. It acts as an obvious flow field of large-scale convergence that is conducive to the development of disturbance and closely related to the formation of TCs[1]. Based on a mean latitude of ITCZ averaged over a 20-year period (1965–1984), Ke and Huang[30] argued that the ITCZ stays around 14° N starting from June, shifts northward to about 19° N in August and retreats southward to around 14° N again in September. Corresponding to its monthly distribution (Fig. 7), the RI has the smallest sample in August, possibly due to the fact that the ITCZ moves so close to the continent of southern China that the TC cannot develop fully. For the mean latitude, the RI sample is 15.42° N and therefore closer to the mean latitude of ITCZ than the SI case (16.27° N), suggesting possible links between the RI and ITCZ and its north-south shifts.

A number of studies[7, 14, 20, 27] have pointed out that large vertical shear is not conducive to the development and strengthening of the TC. Significant differences exist in the variables of VWS5 and VWS7 with both the RI and SI cases, with the latter having the most difference ($\alpha=0.01$). For the RI cases, VWS5 and VWS7 are relatively small, being 7.37 m/s

and 6.95 m/s, respectively, and smaller than the averages of the SI cases by 1.08 m/s and 1.65 m/s, respectively. The argument was verified to some extent. Specifically, VWS5 is lower than 10 m/s in 74% of the RI cases (Fig. 8e), VWS7 is lower than 10 m/s in 68% of the SI cases, and VWS7 is lower than 8 m/s in 64% and 49% in the RI and SI cases, respectively (Fig. 8f). However, some of the RI cases are relatively large in VWS5 and VWS7, with VWS5 higher than 12 m/s in 14% of the cases and VWS7 higher than 14 m/s in 21% of the cases. For the same VWS5 and VWS7 values, the SI cases have corresponding 21% and 32% respectively. According to Zeng et al.[27], a mature and powerful TC possesses deep cyclonic circulation and intense convection, which are able to offset, to some extent, the inhibiting effect of vertical wind shear on its development. In fact, it is necessary to include other factors, such as the scale, intensity and latitude of the TC, to consider the intensity change comprehensively[31].

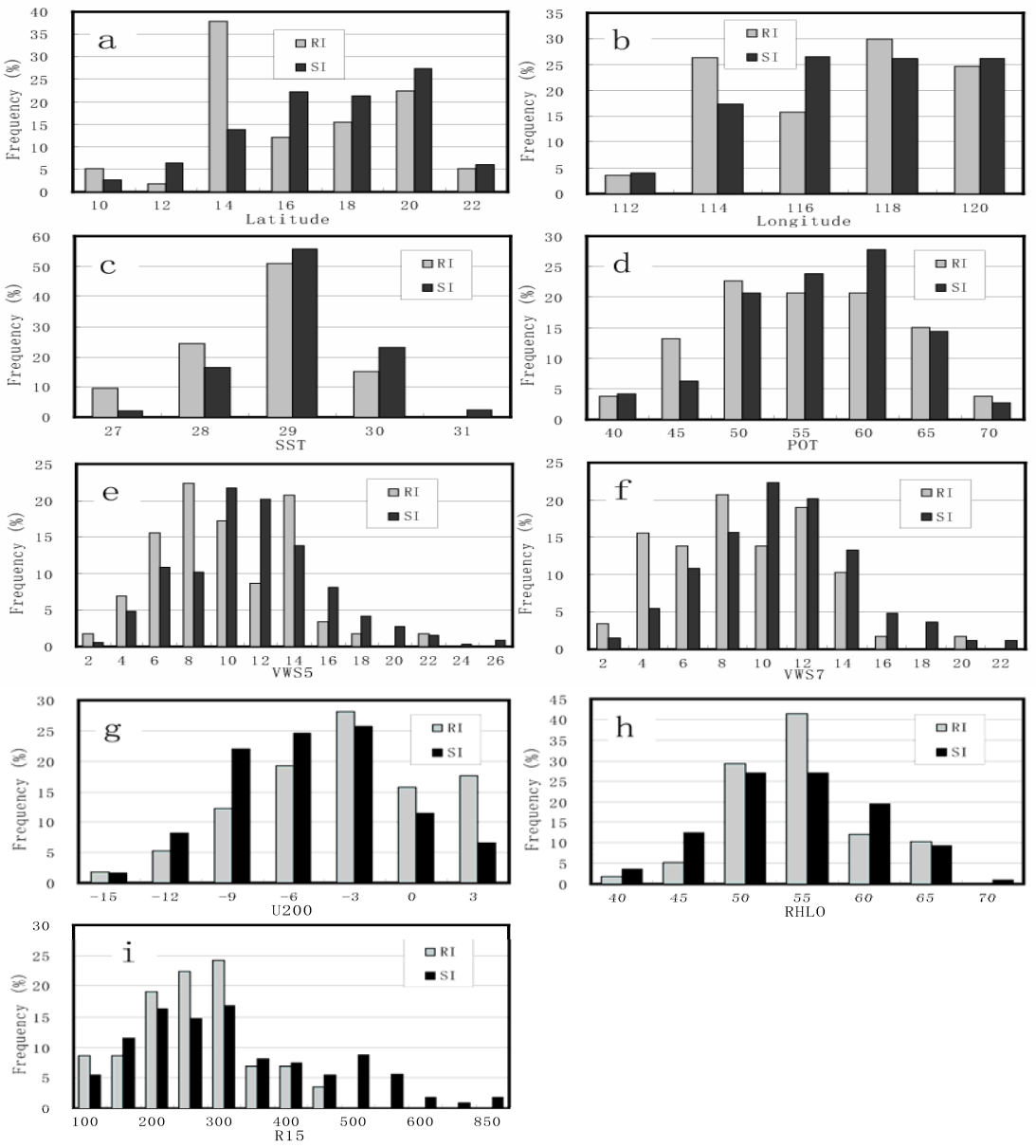

Fig. 8. Distribution of frequency of individual factors for the RI and SI cases at the initial time (t=0 h). Captions about the number of cases follow those of Table 6. a. LAT; b. LON; c. SST; d. POT; e. VWS5; f. VWS7; g. U200; h. RHLO; i. R15.

Compared to the SI cases, RI has a weaker U200 component, with the mean value at -4.67 m/s, difference of mean value at 1.73 m/s, and a small amount of cases of westerly wind (Fig. 8g). According to a statistical study of the Atlantic hurricanes, however, the easterly component is significant in the RI cases while the westerly component is strong in non-RI cases[14]. The statistical study includes only the subtropical cases while cases in this study focus on the TCs affecting the SCS. The difference in the results are attributed to the fact that westerlies prevail in the subtropical upper level in the Northern

Hemisphere while easterlies dominate in the tropics[1]. Besides, r=-0.60, a correlation coefficient derived by computing U200 and VWS7, correlates well linearly[14], suggesting that the larger the easterly component, the larger the vertical shear.

Possibly due to the fact that the SCS is a tropical sea where air-sea interactions are significant and temperature and humidity stay relatively high the year round, no significant differences in the RHLO are found between the two types of cases[29]. The RI cases have a mean RHLO value of 72.08%, just slightly higher than the SI average by 0.67%; there are 64% and 57% of RI and SI cases with the RHLO higher than 50%, respectively (Fig. 8h).

The significance level is the highest for the difference in the 15.4 m/s wind radius (R15). The RI case has a mean value of 231.6 km and the SI case has a mean value of 281.7 m/s, with 83% of the RI cases and 63% of the SI cases having a radius less than 300 km, and 3% of the RI cases and 24% of the SI cases having a radius larger than 400 km (Fig. 8i). Willoughby et al.[32] argued that the contraction of the largest wind-speed radius near the eyewall could lead to rapid changes in the TC intensity. Although the RSMC data cannot be directly used to depict the characteristics of the inner-core wind radii with the RI cases of the SCS, the fact that the R15 is relatively small in the RI cases is sufficient proof that the TC circulation is quite compact.

5 CONCLUSIONS

(1) For most of the TC life cycle, the rate of intensity change is moderate. Most of the TS and STS cases are of the strengthening and stable types while the TY is dominantly in the weakening group. The stronger the initial intensity, the less the observation of strengthening TCs and the smaller the rate of change will be; the more the observation of weakening TCs, the larger the rate of change will be.

(2) The strengthening TCs have the most cases with the largest strengthening rate at 0000 UTC; the weakening TCs have the most cases with the largest weakening rate at 1200 UTC. In general, the rate of weakening is larger with the TY than with the TS and STS.

(3) In the strengthening state, the TS cases are mostly distributed in northeastern SCS, the STS cases in central and eastern SCS, and the TY cases in central SCS. The weakening cases are mostly observed in Hainan Island and the waters east off Vietnam and west off the Philippines. The effects of the TS as well as temperature, cold air and other factors on the TCs are to be discussed further in our future work.

Acknowledgements: We are especially grateful toward the RSMC Tokyo for free download of the data and Professor WANG Ji-zhi at the National Meteorological Center and Chief Forecaster YANG Gui-ming for their invaluable advices on this work.

REFERENCES:

[1] CHEN Lian-shou, DING Yi-hui. An Introduction to the Typhoons in West Pacific [M]. Beijing: Science Press, 1979: 1-491.
[2] DUAN Yi-hong, YU Hui, WU Rong-sheng. Review of the research in the intensity change of tropical cyclone [J]. Acta Meteor. Sinica (in Chinese), 2005, 63(5): 636-645.
[3] YU Hui, DUAN Yi-hong. A statistical analysis on intensity change of tropical cyclone over northwestern Pacific [J]. Acta Meteor. Sinica (in Chinese), 2002, 60(6): 680-687.
[4] YU Yu-bin, YAO Xiu-ping. A statistical analysis on intensity change of tropical cyclone over northwestern Pacific [J]. J. Trop. Meteor. (in Chinese), 2006, 22(6): 521-526.
[5] LI Ying, CHEN Lian-shou, ZHANG Sheng-jun. Statistical characteristics of tropical cyclone making landfalls on China [J]. J. Trop. Meteor. (in Chinese), 2004, 20(1): 14-23.
[6] YUAN Jin-nan, LIN Ai-lan, LIU Chun-xia. Change characters of tropical cyclones with different intensities over the western North Pacific during the last 60 years [J]. Acta Meteor. Sinica (in Chinese), 2008, 66(2): 213-223.
[7] TITLEY D W, ELSBERRY R L. Large intensity changes in tropical cyclones: A case study of supertyphoon Flo during TCM-90 [J]. Mon. Wea. Rev., 2000, 128(10): 3 556-3 573.
[8] HOLLIDAY C R, THOMPSON A H. Climatological characteristics of rapidly intensifying typhoons [J]. Mon. Wea. Rev., 1979, 107(8): 1 022-1 034.
[9] CHEN Qian-jin. A statistical study of the relationship between rapidly intensifying Typhoon eye structure and environmental offshore China [J]. Acta Oceanol. Sinica (in Chinese), 1996, 18(3): 121-127.
[10] LIU Chun-xia, RONG Guang-xun. The climatic analysis of the relationship between the explosive development of typhoon and its environment flow field [J]. J. Trop. Meteor. (in Chinese) , 1995, 11(1): 51-56.
[11] FENG Jin-quan, CHEN Duo. Analyses of climatic characteristics accompanying sudden intensity changes in offshore tropical cyclones in China [J]. J. Trop. Meteor. (in Chinese), 1995, 11(1): 35-42.
[12] YAN Jun-yue, ZHANG Xiu-zhi, LI Jiang-long. Climate characteristics of rapidly intensifying tropical cyclones in the northwest Pacific ocean west of 135° E [J]. J. Trop. Meteor. (in Chinese), 1997, 13(4): 297-305.
[13] WU Da-ming. The climatological characteristics of rapid change of the intensity of the tropical cyclone of the western North Pacific Ocean [J]. Chin. J. Atmos. Sci. (in Chinese), 1997, 21(2): 192-198.
[14] KAPLAN J, DeMARIA M. Large-scale characteristics of rapidly intensifying tropical cyclones in the North Atlantic Basin [J]. Wea. Forecasting, 2003, 18(6): 1 093-1 108.
[15] LIU Chun-xia, RONG Guang-xun. On diagnostic analysis of energy fields of abrupt intensification of typhoon offshore [J]. J. Trop. Meteor. (in Chinese), 1996, 12(2): 174-180.
[16] SHOU Shao-wen, YAO Xiu-ping. A diagnostic study of the composite ambient fields of the explosively developing typhoons [J]. Chin. J. Atmos. Sci. (in Chinese), 1995, 19(4): 487-493.
[17] VENTHAM J D, WANG B. Large-scale flow patterns and their influence on the intensification rates of western North Pacific tropical storms [J]. Mon. Wea. Rev., 2007, 135(3): 1

110-1 127.
[18] LIANG Jian-ying, CHEN Zi-tong, WAN Qi-lin, et al. Diagnostic analysis of the landfall process tropical cyclone "Vongfong" [J]. J. Trop. Meteor. (in Chinese), 2003, 19 (suppl.): 45-55.
[19] HU Chun-mei, DUAN Yi-hong, YU Hui, et al. The diagnostic analysis of the rapid change in tropical cyclones intensity before landfall in South China [J]. J. Trop. Meteor. (in Chinese), 2005, 21(4): 377-382.
[20] YUAN Jin-nan, WANG Dong-xiao, WAN Qi-lin, et al. A 28-year climatological analysis of size parameters for northwestern Pacific tropical cyclones [J]. Adv. Atmos. Sci., 2007, 24(1): 24-34.
[21] YAN Jun-yue, ZHANG Xiu-zhi, CHEN Qian-jin, et al. The standard of rapidly intensified tropical cyclones [J]. Meteor. Mon. (in Chinese), 1995, 21(5): 9-13.
[22] YU Hui, HU Chun-mei, JIANG Le-yi. Comparison of three tropical cyclone strength datasets [J]. Acta Meteor. Sinica (in Chinese), 2006, 64(3): 357-363.
[23] KALNAY E, KANAMITSU M, KISTLER R, et al. The NCEP/NCAR 40-Year Reanalysis Project [J]. Bull. Amer. Meteor. Soc., 1996, 77(3): 437-471.
[24] REYNOLDS R W, RAYNER N A, SMITH T M, et al. An improved in situ and satellite SST analysis for climate [J]. J. Climate, 2002, 15(13): 1 609-1 625.
[25] WEI Feng-ying. Modern diagnosis and prediction technique for climate statistics [M]. Beijing: China Meteorological Press (in Chinese), 2007, 1-296.
[26] YU Yu-bin, YANG Chang-xian, YAO Xiu-ping. The vertical structure characteristics analysis on abrupt intensity change of tropical cyclone over the offshore of China [J]. Chin. J. Atmos. Sci. (in Chinese), 2007, 31(5): 876-886.
[27] ZENG Z, WANG Y, WU C C. Environmental dynamical control of tropical cyclone intensity—an observational study [J]. Mon. Wea. Rev., 2007, 135(1): 38-59.
[28] HANLEY D E, MOLINARI J, KEYSER D. A composite study of the interactions between tropical cyclones and upper-tropospheric troughs [J]. Mon. Wea. Rev., 2001, 129(10): 2 570-2 584.
[29] LIANG Bi-qi. Systems of Tropical Atmospheric Circulation in South China Sea [M]. Beijing: China Meteorological Press, 1991: 1-244.
[30] KE Shi-zhao, HUANG Zhi-hui. On the climatological ITCZ over the area of South China Sea and west Pacific Ocean [J]. J. Trop. Meteor. (in Chinese), 1993, 9(1): 20-27.
[31] DEMARIA M. The effect of vertical shear on tropical cyclone intensity change [J]. J. Atmos. Sci., 1996, 53(14): 2 076-2 087.
[32] WILLOUGHBY, H E, CLOS J A, SHOREIBAH M G. Concentric eyewalls, secondary wind maxima, and the evolution of the hurricane vortex [J]. J. Atmos. Sci., 1982, 39(2): 395-411.

Citation: LI Xun, ZHAO Sheng-rong, LI Ze-chun et al. Characteristics of intensity change in tropical cyclones affecting the South China Sea from 1977 to 2007. *J. Trop. Meteor.*, 2011, 17(2): 156-165.